Interaction of Multipactor Discharge and rf Circuit

R. Kishek and Y. Y. Lau
Department of Nuclear Engineering, University of Michigan, Ann Arbor, Michigan 48109-2104
(Received 30 March 1995)

A simple model is constructed to analyze the temporal evolution of a multipactor discharge in an rf cavity. The multipactor current may, transiently, reach a level comparable to the wall current that is needed to sustain the rf field. It saturates at a much lower level in the steady state, primarily by its loading of the cavity; the image space charge force associated with the multipactor electrons plays a relatively minor role. At saturation, the electron impact energy is equal the lowest value that gives unity in the secondary electron yield curve.

PACS numbers: 85.10.Jz, 52.80.–s, 84.30.Ey

Multipactor is a well-know phenomenon of rf breakdown in microwave cavities, windows, satellite rf payloads, and accelerator structures [1–3]. When an ac electric field exists across a gap, an electron from one surface is accelerated toward the other surface, the impact upon which may release more than one electron by secondary emission. It is easy to see that if the electron transit time across the gap is equal to half of the rf period, a resonant discharge could result.

There exists only very few theoretical analyses of multipactor, most of which concentrate on the response of a single electron to an imposed rf electric field. Analytic expressions have been derived for the phase of the emitted electron and the range of the rf electric field in which a stable, steady-state multipactor may exist [1,4]. While some calculations have included the space charge effects associated with the multipactor electrons [4,5], they omit the important processes of loading and detuning of the rf cavities as the multipactor current grows [2]. In this paper, we use a simple model to address these issues, the analysis of which yields interesting information on the multipactor saturation level, the saturation mechanism, the time scale over which multipactor evolves, and possibly the drastic transient growth of multipactor current before the steady-state solution is reached.

For simplicity, we shall use a one-dimensional model where the multipactor occurs inside a planar gap (Fig. 1). The gap separation is D and the gap voltage is $V_g(t)$. The multipactor discharge is modeled by a single electron sheet of surface density σ that moves across this gap. Upon impact on a gap surface, a new electron sheet is generated by secondary emission. We assume that the voltage V_g that drives the multipactor is provided by an rf cavity. This cavity is modeled by an *RLC* circuit (Fig. 1), with a corresponding quality factor Q and characteristic frequency $\omega_0 = 1/\sqrt{LC}$. As the multipactor electron sheet moves inside the gap, it induces a wall current $I_m(t)$, which loads the *RLC* circuit. Thus, the present model allows for the progressive loading and detuning of the cavity as the multipactor current builds up (Fig. 1). This loading in turn modifies the electron's energy and phase at impact.

Hereafter, we shall use dimensionless quantities with the following normalization scales: D for distance, ω_0 for frequency, $1/\omega_0$ for time, $v = \omega_0 D$ for velocity, $U = mv^2$ for energy, $V = U/e$ for voltage, $E = V/D$ for electric field, $\Sigma = \varepsilon_0 E$ for surface charge density, and V/Z for current. Here, m is the electron mass, $e = 1.602 \times 10^{-19}$ C, ε_0 is the free space permittivity, and $Z = \sqrt{L/C}$ is the intrinsic impedance of the *RLC* circuit. The *RLC* circuit is driven by the normalized ideal current source I_d, and by the multipactor current I_m. Its normalized gap voltage V_g evolves according to the circuit equation (Fig. 1):

$$\left(\frac{d^2}{dt^2} + \frac{1}{Q}\frac{d}{dt} + 1\right)V_g(t) = \frac{d}{dt}[I_{d0}\sin(\omega t + \phi) + I_m(t)], \quad (1)$$

where I_{d0} is the amplitude of the driver current of normalized frequency ω and ϕ is the phase at time $t = 0$. We set $\omega = 1$ in this paper (i.e., resonantly driven).

The normalized multipactor current I_m is given by

$$I_m(t) = -\sigma(t)\frac{dx(t)}{dt}, \quad (2)$$

where σ is always positive, by convention. Equation (2) accounts for the induced current as a result of the motion of the electron sheet within the gap, $0 < x < 1$. It is this term that is solely responsible for the nonlinear

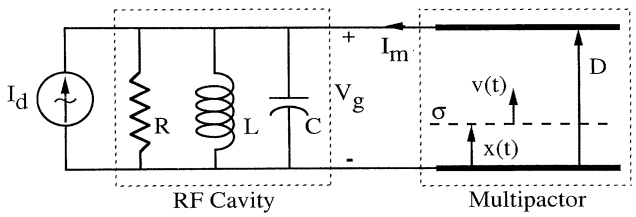

FIG. 1. Model of interaction between rf cavity and multipactor discharge.

 0031-9007/95/75(6)/1218(4)$06.00 © 1995 The American Physical Society

beam loading and frequency detuning of the cavity by the multipactor, as readily seen from Eq. (1) and Fig. 1.

During its transit across the gap, the electron sheet is accelerated according to the normalized force law,

$$\frac{d^2x}{dt^2} = V_g + \sigma(x - \tfrac{1}{2}), \tag{3}$$

where the first term on the right-hand side represents the force due to the gap voltage and the second term the force due to the image charge (of the multipacting electron sheet) on the plates [6].

On impact with a plate at time t_i, the incident electron sheet is removed and a new sheet of surface charge is released by secondary emission. The postimpact surface charge density $\sigma(t_i^+)$ is related to the preimpact charge density $\sigma(t_i^-)$ by

$$\sigma(t_i^+) = \delta\sigma(t_i^-), \tag{4}$$

where δ is the coefficient of secondary emission which depends on the electron impact energy E_i. Here $E_i = (dx/dt)^2/2$, evaluated at $t = t_i^-$. For simplicity, we adopt Vaughan's empirical formula [7] for δ:

$$\delta = \delta(E_i) \cong \delta_{\max}(we^{1-w})^k. \tag{5}$$

In Eq. (5), $\delta_{\max}$ is the maximum value of δ, $w = E_i/E_{\max}$, $E_{\max}$ being the impact energy which yields $\delta_{\max}$, and $k = 0.62$ for $w < 1$ and $k = 0.25$ for $w > 1$. Equation (5) is plotted in Fig. 2, which shows that $\delta = 1$ at two values of impact energies, E_1 and E_2. The lower energy E_1 is designated as the "first crossover point." For simplicity, in writing Eq. (5), we have ignored the (small) threshold impact energy that is required for $\delta > 0$.

We have established analytically the necessary conditions for the existence of steady-state solutions according to Eqs. (1)–(5). These calculations are in a number of ways similar to those given by Riyopoulos, Chernin, and Dialetis [4]. Here we present the numerical results which show the evolution of the multipactor toward these steady-state solutions.

To reduce the number of parameters, we assume that the driver current I_d has been turned on for all time so that the cavity is already filled with rf for $t < 0$. The multipactor current is "turned on" at $t = 0$, in the form of an electron sheet with an initial surface charge density σ_0 that is released from the plate $x = 0$, with zero velocity [8]. We assign a sufficiently low value of σ_0 to observe the buildup of the multipactor current. The initial phase ϕ [Eq. (1)] at which σ_0 is launched is chosen so that this initial electron sheet strikes the other plate in about half an rf cycle. In most cases we run, the precise values of these initial data are not critical. Our simulations thus far have been restricted to a two-surface, first-order multipactor [1], i.e., an electron released from one surface always strikes the other surface without momentarily stopping within the gap. The major free parameters are Q and I_{d0}, after having fixed $\delta_{\max} = 1.2$, $E_{\max} = 0.36$, and $\omega = 1$. (In dimensional units, if the rf cavity has a natural frequency of 1 GHz and a gap separation of 0.22 cm, over which multipactor occurs, these parameters correspond to an ideal rf driver current exactly at 1 GHz, the first crossover point $E_1 = 166$ eV, and δ reaches a maximum value of 1.2 when the impact energy is $E_{\max} = 400$ eV.)

Shown in Fig. 3(a) is the multipactor current, monitored at impact in units of the driver current amplitude I_{d0}, for $Q = 1, 10, 100, 1000$. The very low value of Q, e.g., $Q = 1$, is included in our study to show the trend of the multipactor in a nonresonant structure—one that is relatively immune to beam loading, such as a window.

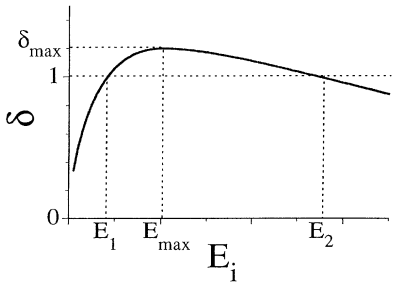

FIG. 2. Secondary electron yield δ as a function of impact energy E_i.

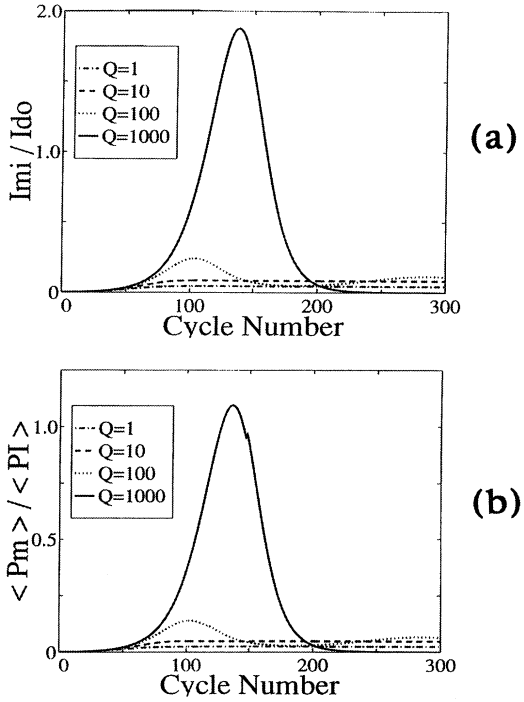

FIG. 3. (a) Transient evolution of multipactor current at impact, in units of the drive current amplitude I_{d0}, for various values of quality factor Q. (b) Time history of the power consumed by multipactor, in units of the input power, at various values of Q.

In all of these runs, we fix the peak rf gap voltage at a value of 0.3 prior to $t = 0$. The fraction of rf power consumed by the multipactor, $\langle -V_g I_m \rangle / \langle V_g I_d \rangle$, is shown in Fig. 3(b). Here $\langle\,\rangle$ denotes the average over the transit time of an electron. Note that in a high Q cavity, *transiently,* the multipactor current may reach a level higher than the drive current I_d [Fig. 3(a)], and at the same time draw much of the power provided by the external source [Fig. 3(b)]. Alternatively, the rf energy stored in a high Q cavity is capable of driving the multipactor current to a large amplitude when the condition becomes favorable. In this regard, it is interesting to recall the well-known fact [1,2] that the multipactor can deposit considerable energy into a tiny spot, and, as a result, causes significant damage to the surface.

The fact that the curves for the multipactor current [Fig. 3(a)] follow the corresponding ones for power dissipation [Fig. 3(b)] suggests that a multipactor discharge behaves a lot more resistively than reactively, even during its nonlinear, transient interaction with the rf circuit. Note, however, that the equivalent resistance is a function of time, since the multipactor current may change over a wide range, as shown in the $Q = 1000$ case in Fig. 3(a), while the gap voltage remains relatively constant during the buildup of the multipactor current [Fig. 4(a)]. For each curve displayed in Fig. 3, a steady state is indeed reached after a sufficiently long time (longer than that shown in Fig. 3 for the $Q = 100$ and $Q = 1000$ cases). In these runs, regardless of the values of Q, the steady-state multipactor current ranges between 5% and 10% of the driver current. Thus, if 20 W of rf power would be required to maintain a steady gap voltage on the order of 300 V, the steady-state multipactor would consume about 2–4 W. However, for a high Q cavity, all 20 W of external power may transiently go to the multipactor. If the spatial extent of the multipactor region is very small, the power density delivered to the gap surface by the multipactor electrons could be very high (see Ref. [10]).

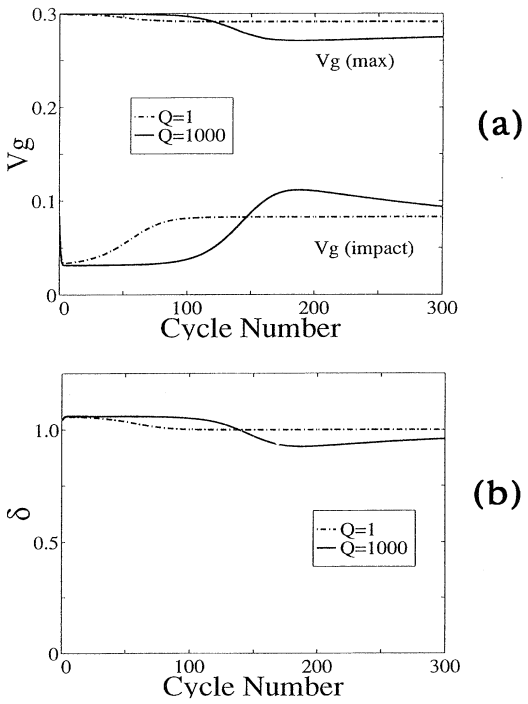

FIG. 4. (a) Evolution of the peak gap voltage V_g(max) and of the gap voltage at the instant of electron impact V_g(impact) for $Q = 1$ and $Q = 1000$. (b) Evolution of the secondary electron yield δ at the instant of electron impact.

Throughout the transient development of the multipactor, the peak rf gap voltage in each cycle changes relatively little, for either the $Q = 1$ case or the $Q = 1000$ case [Fig. 4(a)]. The secondary emission coefficient δ also stays around unity [Fig. 4(b)], in fact, in the vicinity of the first crossover point (E_1) in Fig. 2. A simple physical argument shows that only the first crossover point E_1 in Fig. 2 gives the stable steady-state solution [9]. Our numerical results show that the impact energy indeed approaches E_1 asymptotically in time. We have spot checked that the steady-state values of the gap voltage, of the electron impact phase in the rf cycle, and of the surface charge density are all in good agreement with those obtained from our analytic formulation.

In the present formulation, multipactor affects its own evolution in two ways: through its "beam loading" of the cavity [described by I_m in Eq. (1)] and through the image space charge force [described by the last term in Eq. (3)]. It turns out that as long as $Q \gtrsim 10$, the beam loading effect is far more important than the space charge force in determining the saturation level of the multipactor current [10]. The disparity of their relative importance becomes increasingly more pronounced as Q increases, as high Q cavities can be more readily loaded by a multipactor current. This also explains the sensitivity in the high Q cavities, as exhibited in Fig. 3. This figure gives the tantalizing clue that, in reality, the rf energy stored in high Q cavities may relax via a multipactor discharge, albeit transiently in time, and locally in space [10].

While the above rudimentary analysis provides some quantifications on the temporal evolution of multipactor, we have not really addressed other theoretical issues involving the accessibility of the steady-state multipactor solutions, the possible conversions from the first order to higher order multipactors, and the mutual interactions among multiple electron sheets [1,4]. It must also be remembered that the multipactor is known to depend a great deal on the geometry, on the processing and conditioning of the rf structure, on the cleanliness and condition of the surface, on the duration and power level of the rf pulse, on the external magnetic field, etc. Nevertheless, our simple model does yield the following conclusions: (a) Steady-state multipactor discharge occurs when the rf voltage is of the order of the first crossover energy (E_1

in Fig. 2), confirming the prevailing notion that the multipactor is a low to medium voltage phenomenon. (b) It saturates in an rf cavity as a result of loading; the image space charge force of the multipacting electrons is insignificant to alter the phase condition or the saturation condition whenever $Q \gtrsim 10$. (c) The rf energy stored in a high-Q cavity may lead to a large buildup of multipactor current in a transient manner. (d) There is phase focusing for the multipactor, as numerically demonstrated when the assigned initial phase in the simulation is removed from the optimal value. (e) The peak gap voltage need not be appreciably reduced during the buildup of the multipactor current.

We have benefited from many useful conversations with David Chernin, Spilios Riyopoulos, Perry Wilson, Jake Haimson, Ronald Gilgenbach, and Richard Briggs. This work was supported by NRL/ONR.

[1] J. R. M. Vaughan, IEEE Trans. Electron Devices **35**, 1172 (1988).

[2] A. S. Gilmore, *Microwave Tubes* (Artech House, Norwood, MA, 1986), p. 474.

[3] G. A. Loew and J. W. Wang, SLAC Report No. 4647, 1988; A. D. Woode and J. Petit, Microwave Journal **35**, 142 (1992).

[4] S. Riyopoulos, D. Chernin, and D. Dialetis, Phys. Plasmas **2**, 3194 (1995).

[5] F. M. Mako and W. Peter, in *Proceedings of the 1993 IEEE Particle Accelerator Conference, Washington, DC, 1993* (IEEE, New York, 1993), p. 2702.

[6] The force law, Eq. (3), may easily be modified to include a transverse magnetic field. We have extensively studied such cases; the findings will be published elsewhere.

[7] J. R. M. Vaughan, IEEE Trans. Electron Devices **36**, 1963 (1989); A. Shih and C. Hor, IEEE Trans. Electron Devices **40**, 824 (1993).

[8] It is shown by Riyopoulos, Chernin, and Dialetis [4] that the inclusion of the initial velocity of the secondary electrons does not qualitatively change their steady-state solutions.

[9] If the impact energy E_i is greater (less) than the first crossover point E_1, more (fewer) electrons will be released by secondary emission. As a result, more (less) energy will be drained from the cavity as it accelerates more (fewer) secondary electrons. This leads to a lower (higher) gap voltage which makes E_i closer to E_1 in subsequent cycles. Thus E_1 is a stable steady-state solution. A similar argument shows that the second crossover point, E_2 in Fig. 2, is unstable.

[10] When the space charge effect is ignored, the analysis given in this paper may actually be applied to a "blob" of multipactor electrons, of total charge $-q_m$, that is *very localized* in space (instead of an electron *sheet* shown in Fig. 1). This is because the induced current I_m is simply $-q_m d(x/D)/dt$ by Ramo's theorem [see, e.g., Chapter 1 of C. K. Birdsall and W. B. Bridges, *Electron Dynamics of Diode Regions* (Academic, New York, 1966)]. Thus, in Eqs. (2) and (4), σ may be taken to represent this localized blob of multipactor electrons. In Eq. (3), σ is set to zero when "the space charge effect" is ignored. Equations (1) and (5) are unchanged.